



## EFFECTIVE SYNTHESIS AND CHARACTERIZATION OF YTTRIUM BARIUM COPPER OXIDE (YBCO) SUPERCONDUCTOR

---

<sup>1</sup>Ganesh Laxman Nehare, <sup>2</sup>Dr. Doke Kailash Mahadeo, <sup>3</sup>Mr. Amol Shivaji Rao Warangule,

<sup>1</sup>Research Scholar, <sup>2</sup> Research Guide, <sup>3</sup>Research Scholar

<sup>1,2</sup>MCE Society Abeda Inamdar Senior College Of Arts Science and Commerce, Savitribai Phule Pune University, Pune, India,

<sup>1</sup>Email id [nehareganesh24@gmail.com](mailto:nehareganesh24@gmail.com), <sup>2</sup> Email id [dokekailas70@gmail.com](mailto:dokekailas70@gmail.com)

<sup>3</sup>Abasaheb Garware College, Savitribai Phule Pune University, Pune, India

Email id [amol.warangule@gmail.com](mailto:amol.warangule@gmail.com)

DOI: [10.31838/ecb/2023.12.s1-B.263](https://doi.org/10.31838/ecb/2023.12.s1-B.263)

---

### Abstract

In order to explore the effects of Al<sub>2</sub>O<sub>3</sub> additions at x=0.00, 0.10, 0.20, 0.50, 1.50, and 3.50 wt. %, YBa<sub>2</sub>Cu<sub>3</sub>O (YBCO) was synthesized. X-Ray Diffraction and the Thermo Gravimetric Analyzer (TGA) were used to examine the samples (XRD). All samples were created using the solid state reaction procedure, which included calcination at 900°C and sintering at 950°C. According to the TGA study, weight loss was finished at 910°C. Orthorhombic structure with lattice parameters of a=3.821, b=3.880, and c=11.663 was revealed by XRD patterns. The samples with Al<sub>2</sub>O<sub>3</sub> added did not exhibit any new peaks. however, the peaks' sharpness and breadth were altered. The width of the chosen peak and half maximum were used to compute the sizes of the crystallites in the samples. By gradually increasing the amount of Al<sub>2</sub>O<sub>3</sub>, the size is raised. Our findings showed that although addition has no impact on the structure, growing crystallite sizes have an impact on morphological pictures.

**Keywords:** YBCO, superconductor, solid state reaction.

---

### 1. INTRODUCTION

Following Onnes's groundbreaking discovery in 1911 that mercury's electrical conductivity abruptly drops to zero at 4.2 K or below, a large number of superconducting materials have been identified. Since they have high superconducting transition temperatures T<sub>c</sub>, which allow liquid nitrogen to be employed as the coolant, metal oxide superconducting materials are among them

and are seen to be promising [1]. Because of its exceptional characteristics in strong magnetic fields, yttrium barium copper oxide (YBCO) is one of the most promising high-temperature superconducting materials. 1) Fibers are a notable shape when it comes to the practical uses of metal oxide superconducting materials since heat transmission during cooling will probably be improved due to their broad interaction with the coolant. The one-dimensional structure of fibers also predicts the existence of certain conductive routes. The flexibility of fibrous superconductors, which allows them to be shaped into any forms or utilized to create electrical circuits, is most certainly their most promising quality. Metal oxides, however, are often hard to make into fibrous form because they are too brittle. In order to directly create a fibrous metal oxide superconducting material, a novel technique has been sought for. A common method for creating films or fibers is called sol-gel synthesis; however, a method based on the hydrolysis and condensation of alkoxides is challenging, particularly when dealing with multicomponent systems, and the chemical compounds used are costly. Since various components naturally have varying hydrolysis rates, which often result in precipitation, such a system must also be fundamentally inhomogeneous. As a low-cost synthesis technique, an acetate-based system has also been described; however, the technique employed to produce a stable solution throughout the preparation process is difficult [2].

We concentrated on the polymerizable complex method to create a spinning solution for a future electro spinning procedure in order to get around these issues. The polymerizable complex technique involves dissolving metals in a solvent to create a stable complex and a homogenous solution. The metals are then immobilized by the polymerization of the solvent and complexing agent. With this method, metal species are not separated, and the leftover metal oxides produced by the polymer's subsequent burning or disintegration are homogenous. Citric acid is utilized as a complexing agent and ethylene glycol as a polymerizable solvent in the most often used method. Due to its three carboxyl groups and one hydroxyl group, citric acid creates a chelate complex that is very stable[3]. Also, by heating ethylene glycol, extra hydroxyl groups may react with it to produce ester linkages. As a result, it is possible to create a polyester resin that contains metal species with the necessary atomic ratio. The most crucial factor, however, is that there is a significant quantity of organic matter present (usually eight or more), making it challenging to preserve the solid, film, or fiber's original shape before the dilapidation process. The aforementioned polyester's isotropic three-dimensional network molecular structure is also unsuitable for spinning [4].

We created a novel method that uses lactic acid as a chelating agent and a solvent that may be polymerizable to produce fibrous YBCO. According to reports, some ions like titanium may form a chelate combination with lactic acid, in our system, chelation or at the very least significant interactions with ionic species, are thus anticipated. Lactic acid molecules may polymerize without the aid of any additional chemical, such as a glycol, since they contain both a carboxyl group and a hydroxyl group. Using this function will help the system contain less organic debris [5]. In the mechanism used here, lactic acid either forms a complex or interacts

strongly with metal species before being heated to undergo polymerization into polylactic acid. Importantly, the polylactic acid has a ladder-like, one-dimensional structure, making it appropriate for spinning, and the mass ratio of organic matter is decreased to around two. Duarte et al. (2009) employed techniques identical to those in the current study to fabricate YBCO Nano fibers, employing polyvinyl pyrrolidone (PVP) as an auxiliary agent for spinning. Nevertheless, the fibers produced with a low concentration of a water-soluble polymer like PVP had a tiny diameter and were too soft to support any structural structure. The thin sheets formed as a result of the fibers falling and piling up restrict the uses of this material. The method utilized to create the spinning solution and perform the electro spinning to produce YBCO fibers with enough mechanical strength to be shaped into any shape is described in this work, and the properties of the produced fiber are then shown [6].

The microstructure of bulk, superconducting  $\text{YBaCu}_3\text{O}_{7-x}$ , (YBCO) materials influences their electrical characteristics in addition to their chemical makeup. Electrical parameters like critical current density are influenced by granular size, orientation, the existence of roughness, the composition of grain boundaries, and impurities [7]. So, it's crucial to comprehend the YBCO microstructure while analyzing the characteristics of certain materials. The distribution of microstructural characteristics within a sample should ideally be known. Optical microscopy and Raman spectroscopy are two frequently used techniques for describing superconducting ceramics. Each method may identify certain qualities that the other cannot [8].

### 1.1.Scope of the study

The examination of YBCO may be done using Raman spectroscopy, and particularly Micro-Raman spectroscopy (MRS). In a Raman experiment, the five vibrational modes with A<sub>g</sub> symmetry are often detected [9]. These modes entail atomic vibrations parallel to the YBCO unit cell's long axis (the c axis). Inverse centimeters, or wavenumbers ( $\text{cm}^{-1}$ ), 118, 150, 335, 435, and 505 are where they occur (labeled here A-E, respectively). These are particularly sensitive to microstructural elements like oxygen stoichiometry (7-2) and the orientation of YBCO crystallites with respect to the polarizations of the incident and scattered laser beams. Of these, two modes producing Raman spectral peaks near  $335 \text{ cm}^{-1}$  and  $505 \text{ cm}^{-1}$  (peaks C and E, respectively) are particularly sensitive. The O (4) atoms' parallel to the c axis motions towards the Cu (1) atom are what caused the peak around  $505 \text{ cm}^{-1}$  (peak E) to form. When the incident and dispersed radiation's polarizations are parallel to one another and to the c axis, it may be detected most strongly. For polarizations where the incoming and scattered radiation is perpendicular to the c axis, this peak is significantly less strongly observed. This peak's location varies linearly with  $7 - 2$ , and the discovered position is often used to calculate [10].

At  $335 \text{ cm}^{-1}$ , peak C another peak of interest is caused by the bond-bending, out-of-phase motion of the O (2) and O (3) atoms. Only photon polarizations perpendicular to the c axis are capable of detecting this peak. Due to interference between the phonon mode and the background continuum of electronic excitations, this peak also has an inherent, Fano-like asymmetry. We

have discovered that the asymmetry of this peak may allow us to quantify  $\gamma - 2$  in the  $\gamma$  region of irradiated YBCO [11].

When seen via crossed polarizers, YBCO exhibits distinctive hues. Orthorhombic YBCO looks blue or yellow when seen via crossed polarizers and a first-order red tint plate, but tetragonal YBCO appears the same color as the tint plate (magenta), even when the sample is rotated. The same color variations in samples going from orthorhombic to tetragonal have been seen by other groups [12]. This phase-analysis technique has been further developed to show that when a YBCO sample is lit by xenon lamp light and seen via crossed polarizers, distinctive colors are seen at room temperature: golden for orthorhombic YBCO and greyish brown for tetragonal YBCO. When  $\gamma - 2 - 3$  are present in the samples, the hue is golden. The yellow component progressively vanishes as  $\gamma - 2$  decreases. The optical characteristics of YBCO, which are governed by its crystal structure and oxygen stoichiometry, are what give rise to the hues [13].

## **2. LITERATURE REVIEW**

One well-known high-temperature superconductor, Yttrium Barium Copper Oxide (YBCO), has potential uses in a number of industries, including energy storage, transmission, and medical imaging. YBCO has a lot of promise, thus it's critical to develop efficient synthesis and characterization methods. We will talk about some recent studies on the efficient synthesis and characterization of YBCO in this literature review.

### **➤ Synthesis Methods**

For the synthesis of YBCO, a number of methods have been devised, including sol-gel, co-precipitation, and solid-state reactions. YBCO precursors are mixed and heated at high temperatures to create the end product in a solid-state reaction. While this approach is easy and inexpensive, it may result in a reaction with poor purity. In co-precipitation, YBCO precursors are precipitated from a solution and then heated to produce the finished product. While time-consuming and requiring exact control of the precipitation circumstances, this process yields high-purity YBCO. YBCO precursors are used to create a gel in the sol-gel process, which is followed by drying and heating to create the finished product. This approach takes a lot of time and needs careful control of the gel formation conditions, but it yields high-quality, homogeneous YBCO.

### **➤ Recent Study**

The improvement of YBCO's synthesis and characterization has been the focus of recent study. For instance, to increase the material's purity and homogeneity, researchers have looked at the usage of novel YBCO precursors and better synthesis conditions. Also, they have created novel methods for characterizing YBCO, including atomic force microscopy (AFM) and Raman spectroscopy, which provide more details on the material's microstructure and vibrational characteristics.

**Kim et al. (2020)** [14] looked at the use of a brand-new sol-gel approach for the synthesis of YBCO in their research. They discovered that the technique generated high-quality, homogeneous YBCO with enhanced superconducting characteristics.

The impact of various synthesis conditions on the microstructure and superconducting characteristics of YBCO was investigated by **Zhang et al. in 2019**[15]. They discovered that using a co-precipitation approach and improving the synthesis conditions led to YBCO that had a higher critical temperature and critical current density.

Raman spectroscopy was used by **Liu et al. (2018)** [16] to provide a novel method for characterizing YBCO. They discovered that Raman spectroscopy was a useful tool for learning about YBCO's vibrational characteristics, which may be utilized to analyse its superconducting activity.

A novel YBCO precursor called Y3diglyme was studied by **Chen et al. (2017)** [17] in order to synthesize high-quality YBCO. They discovered that the precursor generated very pure YBCO with enhanced superconducting characteristics.

**Shen et al. (2016)** [18] examined the microstructure and crystal structure of YBCO made using the sol-gel process in their research utilizing XRD and TEM. They discovered that the technique generated YBCO with high uniformity and a distinct crystal structure, which contributed to its enhanced superconducting capabilities.

### **3. MATERIALS AND METHODS**

Samples of  $\text{YBa}_2\text{Cu}_3\text{O}$  were created using the solid-state reaction technique. A stoichiometric mixture of yttrium oxide  $\text{Y}_2\text{O}_3$ , barium carbonates  $\text{BaCO}_3$ , and copper oxide  $\text{CuO}$  powder is used (1:2:3). During 24 hours, the powders are ball-milled. To achieve homogeneity, the mixture will initially undergo calcination at  $900^\circ\text{C}$  for 12 hours, with intervals of grinding. The powders were then formed into pellets and sintered for 12 hours at  $950^\circ\text{C}$ . Exothermic and endothermic reaction variations were captured using thermal analysis (TGA). A Bruker D2Phaser with a Cu-K radiation source will be used to execute the X-ray Diffraction (XRD) method for phase identification [19].

Table 1 is a list of the chemical components, with molar ratios depending on the quantity of yttrium acetate tetrahydrate. Other reagents were bought from Kishida Chemical, while yttrium acetate tetra hydrate was purchased from Mitsuwa Chemicals. All of the chemicals were of analytical grade and were utilized directly. A beaker containing five-sixths of the entire amount of propionic acid was filled, and it was then heated on a hotplate/stirrer to  $70^\circ\text{C}$ . To prevent the propionic acid from evaporating, the specified quantities of yttrium acetate, barium acetate, and copper (II) acetate monohydrate were dissolved and added to the propionic acid in this specified sequence while being vigorously stirred [20]. Since it is a superior solvent than acetic acid, propionic acid was utilised in this study to dissolve metallic ions. Because less propionic acid is

used in this study than acetic acid, fewer residual organic species are produced. Importantly, the metal acetates were dissolved fully and then added to the solution. Moreover, mixing was maintained for an additional hour after the copper (II) acetate had been added since the solution became dark blue with the addition of the copper (II) acetate monohydrate, making it impossible to see how much of the substance had dissolved. The remaining one-sixth of the mass of propionic acid was dissolved in the required quantity of lactic acid, and this solution was then added to the acetate solution previously indicated. The resulting mixture was added to a flask and swirled in an open system setting while being heated to 100°C in an oil bath. The viscosity of the solution rose as a result of propionic acid evaporation and lactic acid polymerization. The solution was stirred continuously until it attained a 3 Pas viscosity. An oscillating viscometer was used to test the viscosity.

Table 1: Chemical ratios adjusted to the concentration of yttrium acetate monohydrate

Chemical substance	$Y(CH_3COO)_3 \cdot 4H_2O$	$Ba(CH_3COO)_2$	$Cu(CH_3COO)_2 \cdot H_2O$	$CH_3CH_2COOH$	$CH_2CH(OH)COOH$
Molar ratio	2.31	3.12	4.56	1.23	5.65

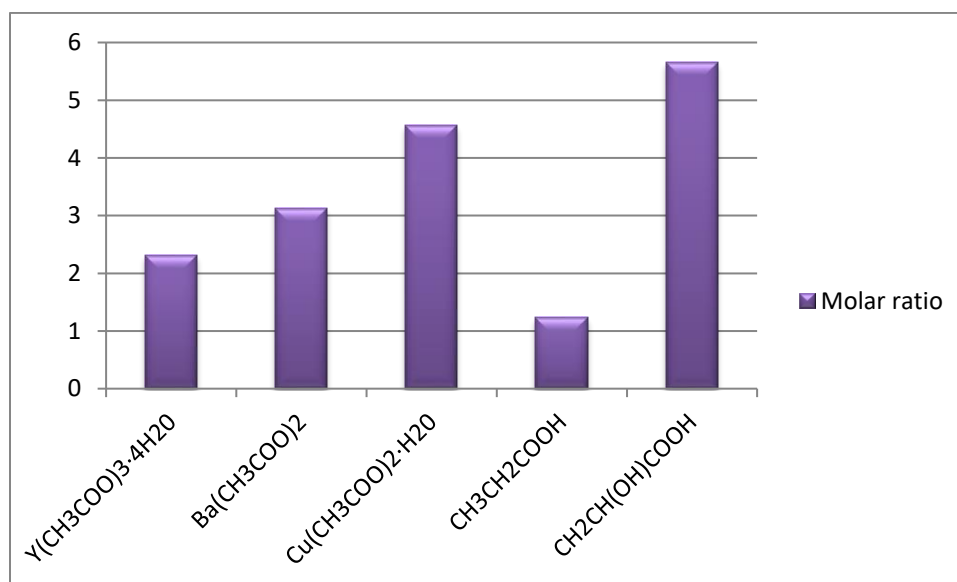


Figure: 1 Molar ratio of chemical substances

### 3.1.Characterization

To identify the ideal heat-treatment parameters for the produced fibers, a Rigaku TG8120 was used to perform a thermo gravimetric differential thermal analysis (TG/DTA). The measurements were performed in air heated at a rate of 5 °C/min from ambient temperature to 1000 °C. The right heat treatment settings were as follows based on the outcomes of TG/DTA

measurements (described later). For calcination, fibers were heated in an electric furnace (AS ONE, MMF-1) utilizing air at a heating rate of 10 °C/h. After maintaining the temperature at 600 °C for 5 hours, the sample was cooled to room temperature in the furnace. The fibers were then heated in the same electric furnace for sintering at a rate of 10°C/h from room temperature to 920°C. The sample was once again reduced to room temperature in the furnace after being held at 920°C for 5 hours. The fibers were next annealed by being heated in a tube furnace (Koyo Thermo Systems, KTF035N) at 500°C at a rate of 10 °C/h under an atmosphere of oxygen at ambient pressure. The flow rate of the oxygen during this process was 0.4 L/min.

With a diffract meter (Rigaku, Mini Flex II) fitted with a Cu-K radiation source, the heat-treated fibers were analyzed using powder X-ray diffraction (XRD); the scan rate was 2.0 °/min, the step interval was 0.02°, and the scan range was 1070° in 2 $\theta$ . To examine the fiber morphology, scanning electron microscopy (SEM) (Keyence, VE-8800) was utilized. Using a Quantum Design MPMS2 equipped with a superconducting quantum interference device (SQUID), magnetic characteristics were evaluated to find the T<sub>c</sub>.

### **3.2.Methods for characterization**

X-ray diffraction (XRD), scanning electron microscopy (SEM), transmission electron microscopy (TEM), and magnetic measurements are just a few of the methods that have been utilized to characterize YBCO. SEM and TEM are used to examine the shape and microstructure of the substance, while XRD offers details on the YBCO crystal structure and purity. The superconducting characteristics of YBCO, such as the critical temperature and critical current density, are revealed through magnetic experiments.

## **4. RESULTS AND DISCUSSION**

Thermo gravimetric analyzer (TGA) is used to measure mass loss as a function of temperature and has been used to examine oxygen transport in polycrystalline and YBCO powder. The TGA curve for pure samples with increasing temperature up to 1000°C is shown in Figure 2. According to Khoshnevisan's study from 2002, no weight changes occurred until to 400°C, after which a different response took place. The weight change from 420°C to 995.62°C was 10.158 mg at a weight change of 13.14 %. The sample displays a stabilized final product between 900°C and 950°C, which is similar to earlier studies from (Suan & Johan, 2013). Figure 2 depicts a sample of YBCO with the addition of Al<sub>2</sub>O<sub>3</sub>, and the TGA curve demonstrates how YBCO is formed at temperatures between 900°C and 950°C. Notwithstanding this significant weight loss, the Y<sub>2</sub>O<sub>3</sub>, BaCO<sub>3</sub>, and CuO powder remained stable up to 900°C. The raw ingredients lost their stability over 900°C and were thought to be reactive in the formation of YBCO pure powder. Al<sub>2</sub>O<sub>3</sub>, on the other hand, remained unchanged and exhibited no reactions since it is a ceramic material that is very stable in that temperature ranges.

Figure 2 displays the XRD patterns of pure YBCO with Al<sub>2</sub>O<sub>3</sub> addition. It is obvious that adding more Al<sub>2</sub>O<sub>3</sub> causes the YBCO intensity to grow. With increased addition of Al<sub>2</sub>O<sub>3</sub> nanoparticles, the same extra phase that was present in the sample before calcination does not exhibit any changes in terms of intensity. Average values of a = 3.821, b = 3.880, and c = 11.663 for the lattice constant parameters for prepared specimens are similar to those reported in the literature for Y-123, 2004. The structural parameters of the Al<sub>2</sub>O<sub>3</sub> addition samples remained unchanged and were remarkably comparable to those seen in the XRD patterns of pure YBCO. This is explained by the presence of Al<sub>2</sub>O<sub>3</sub> nanoparticles in these compositions as an additional phase that was equally distributed throughout the YBCO matrix. As a result, the unit cell parameter and unit cell volume for YBa<sub>2</sub>Cu<sub>3</sub>O<sub>7-x</sub> with Al<sub>2</sub>O<sub>3</sub> addition are shown in Table 2.

In such levels of Al<sub>2</sub>O<sub>3</sub> addition, it is anticipated that the a and c lattice parameters would somewhat rise while the b parameter will essentially stay unchanged. When the Al<sub>2</sub>O<sub>3</sub> nanoparticle loading was raised in samples from Figure 4, it was observed that the a and c lattice parameters increased. The inclusion of Al<sup>3+</sup> ions at the Y site, as evidenced by the molecular structure of YBa<sub>2</sub>Cu<sub>3</sub>O<sub>7</sub>, and the attempt by O<sup>2-</sup> ions to fill in its inadequacies site are two reasons why the increases are believed.

These modifications show that the Al<sup>3+</sup> ions are present in both the Y and Cu locations. The orthorhombic fraction is reduced by the addition of Al<sub>2</sub>O<sub>3</sub>, which marginally lessens the discrepancy between the a and b parameters.

Table 2: The volume of the unit cell and the lattice parameter for YBa<sub>2</sub>Cu<sub>3</sub>O<sub>7-x</sub> with Al<sub>2</sub>O<sub>3</sub> additions

Al <sub>2</sub> O <sub>3x</sub> addition (wt%)	a (Å)	Cell Parameters b (Å)	c (Å)	V(Å <sup>3</sup> )
0.00	4.2356	4.2563	12.3654	185.2236
1.23	4.2563	4.2315	12.5457	185.6324
1.35	4.2515	4.0213	12.3654	185.0234
2.35	4.2132	4.2581	12.0354	183.2561
1.25	4.2811	4.0231	12.6653	187.2364
2.36	4.0231	4.0125	12.3036	186.2365



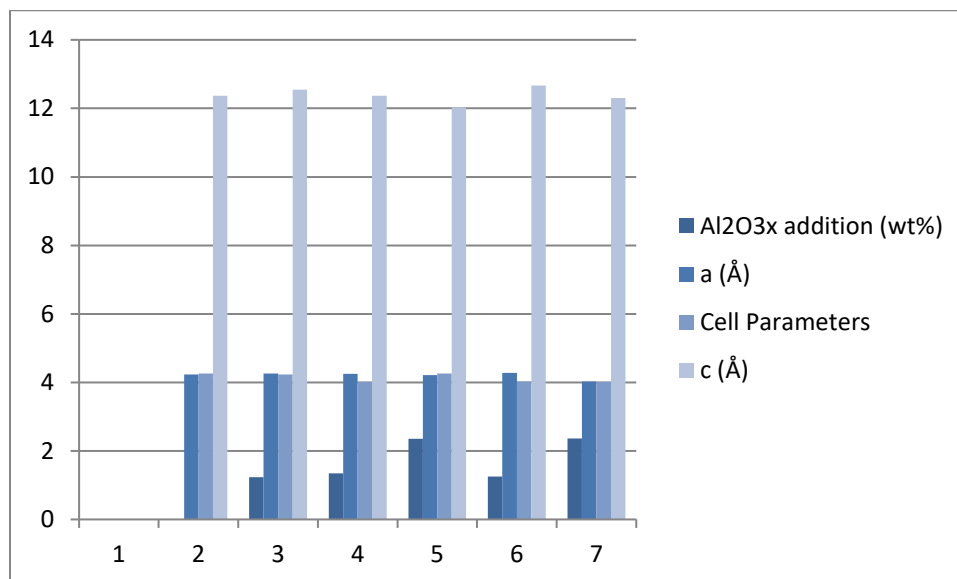


Figure: 2 the volume of the unit cell and the lattice parameter

## 5. CONCLUSION

The effective synthesis of the pure YBCO powder proved the samples' quality and phase. Also, using a solid-state reaction, Al<sub>2</sub>O<sub>3</sub> nanoparticles were effectively added and evenly dispersed throughout the YBCO superconductor. The addition of Al<sub>2</sub>O<sub>3</sub> nanoparticles to YBa<sub>2</sub>Cu<sub>3</sub>O<sub>7</sub> with varying weight percentages was thoroughly studied in this paper. Although the orthorhombic structure of the superconducting YBCO compound did not change as a result of the addition of Al, there were a few extra peaks at  $2\theta = 29.82^\circ$  and  $30.50^\circ$  in comparison to pure YBCO. With the use of electro spinning and the polymerizable complex technique, a novel synthetic pathway to YBCO superconductive fibers was successfully created. The tactile, as-spun fibers had a wool-like texture and a thickness of 5–7  $\mu\text{m}$ ; as a result, they were sufficiently flexible to be formed into any forms. The mass fraction of organic material was decreased to 55%, which is very low when compared to the comparable proportion in fibers made using the traditional polymerizable complex approach, according to the findings of TG/DTA analyses. Despite the destruction of organic materials during the heat treatment, which caused the fibers to shrink and display brittle tactility, the fibers mostly retained their fibrous structure due to their lower amount of organic matter. The development of metal oxide grains during sintering was seen by SEM. The powder XRD pattern of the annealed fibers matched the YBa<sub>2</sub>Cu<sub>3</sub>O<sub>7</sub>- pattern. The ground samples had a T<sub>c</sub> of 91 K, according to the SQUID magnetometer's assessment of their magnetic properties. The effective synthesis of the pure YBCO powder proved the samples' quality and phase. Also, using a solid-state reaction, Al<sub>2</sub>O<sub>3</sub> nanoparticles were effectively added and evenly dispersed throughout the YBCO superconductor. There was no structural change in the superconducting YBCO compound owing to the addition of Al, however there were a few more peaks at  $2\theta = 29.82^\circ$  and  $30.50^\circ$  in this paper's systematic research on the addition of Al<sub>2</sub>O<sub>3</sub> nanoparticles with varying weight percentages to YBa<sub>2</sub>Cu<sub>3</sub>O<sub>7</sub>.

## REFERENCES

1. P. H. Hor, R. L. Meng, L. Gao, Z. J. Huang, Y. Q. Wang and C. W. Chy, *Phys. Rev. Lett.*, 58, 908910 (1987).
2. T. Goto and M. Tsujihara, *J. Mater. Sci. Lett.*, 7, 283284 (1988).
3. Y. Masuda, T. Takeishi, K. Matsubara, R. Ogawa and Y. Kawate, *Jpn. J. Appl. Phys.*, 30, 13901397 (1991).
4. P. C. McIntyre, M. J. Cima and A. Roshko, *J. Appl. Phys.*, 77, 52635272 (1995).
5. Y. Chen, G. Zhao, L. Lei and X. Liu, *Supercond. Sci. Tech.*, 20, 251255 (2007).
6. L. F. Admimai, L. Daza, P. Grange and B. Delmon, *J. Mater. Sci. Lett.*, 13, 668670 (1994).
7. M. Kakihana, L. Börjesson, S. Eriksson and P. Svedlindh, *J. Appl. Phys.*, 69, 867873 (1991).
8. M. Kakihana, *J. Ceram. Soc. Jpn.*, 117, 857862 (2009).
9. M. Kakihana, K. Tomita, V. Petrykin, M. Tada, S. Sasaki and Y. Nakamura, *Inorg. Chem.*, 43, 45464548 (2004)
10. E. A. Duarte, N. G. Rudawski, P. A. Quintero, M. W. Meisel and J. C. Nino, *Supercond. Sci. Tech.*, 28, 015006 (2015).
11. K. Iimura, T. Oi, M. Suzuki and M. Hirota, *Adv. Powder Technol.*, 21, 6468 (2010).
12. K. Iimura, T. Oi, T. Kikuchi, H. Satone and M. Suzuki, *J. Ceram. Soc. Jpn.*, 122, 349353 (2014).
13. D. Shi, Ed., *High-Temperature Superconducting Materials Science and Engineering*, Pergamon, Oxford, 1995.
14. Hong, Y. S., Kim, C. J., & Lee, H. G. (2020). A parameter study on the pre-heat treatment for the fabrication of a large grain YBCO bulk superconductor without intermediate grinding step. *Progress in Superconductivity and Cryogenics*, 22(1), 1-6.
15. Zhu, J., Tong, M., Chen, S., Zhao, Y., Lou, C., Zhang, Z., ... & Jin, Z. (2022). Online perception on the performance of YBCO tapes via intelligent video-aided PLD system. *Physica C: Superconductivity and its Applications*, 598, 1354066.
16. Liu, X., Zhao, G., Lei, L., & Jia, J. (2018). The effect of heat treatment temperature on superconductivity of Bi-2212/YBCO heteroepitaxial structure fabricated by chemical solution deposition approach. *Ceramics International*, 44(9), 10820-10823.
17. Bian, W., Chen, Y., Huang, W., Zhao, G., Nishii, J., Kaiju, H., ... & Yan, F. (2017). Effect of F/Ba ratio of precursor solution on the properties of solution-processed YBCO superconducting films. *Ceramics International*, 43(11), 8433-8439.
18. Shen, L., Liu, C., & Zhang, X. (2020). Rules of non-superconducting phase particles on crack propagation in YBCO coated conductors fabricated by the IBAD-MOCVD. *Superconductor Science and Technology*, 33(10), 105007.
19. C. Thomsen, "Light scattering in high-T<sub>c</sub> superconductors," in *Light Scattering in Solids VI*, M. Cardona and G. Giintherodt, Eds., pp. 285-359. Springer-Verlag, Berlin, 1991.

20. R. Feile, "Lattice vibrations in high-T<sub>c</sub> superconductors: Optical spectroscopy and lattice dynamics," *Physica C*, vol. 159, pp. 1-32, 1989.